Sialylation of N-linked glycans mediates apical delivery of endolyn in MDCK cells via a galectin-9–dependent mechanism

Di Mo[a], Simone A. Costa[b], Gudrun Ihrke[c], Robert T. Youker[a], Nuria Pastor-Soler[a,d], Rebecca P. Hughey[a,d], and Ora A. Weisz[a,d]

[a]Renal Electrolyte Division and [b]Department of Biological Sciences, Carnegie Mellon University, Pittsburgh, PA 15213; [c]Department of Pharmacology, Uniformed Services University School of Medicine, Bethesda, MD 20814; [d]Department of Cell Biology and Physiology, University of Pittsburgh School of Medicine, Pittsburgh, PA 15261

ABSTRACT **The sialomucin endolyn is implicated in adhesion, migration, and differentiation of various cell types. Along rat kidney tubules, endolyn is variously localized to the apical surface and endosomal/lysosomal compartments. Apical delivery of newly synthesized rat endolyn predominates over direct lysosomal delivery in polarized Madin–Darby canine kidney cells. Apical sorting depends on terminal processing of a subset of lumenal N-glycans. Here we dissect the requirements of N-glycan processing for apical targeting and investigate the underlying mechanism. Modulation of glycan branching and subsequent polylactosamine elongation by knockdown of *N*-acetylglucosaminyltransferase III or V had no effect on apical delivery of endolyn. In contrast, combined but not individual knockdown of sialyltransferases ST3Gal-III, ST3Gal-IV, and ST6Gal-I, which together are responsible for addition of α2,3- and α2,6-linked sialic acids on N-glycans, dramatically decreased endolyn surface polarity. Endolyn synthesized in the presence of kifunensine, which blocks terminal N-glycan processing, reduced its interaction with several recombinant canine galectins, and knockdown of galectin-9 (but not galectin-3, -4, or -8) selectively disrupted endolyn polarity. Our data suggest that sialylation enables recognition of endolyn by galectin-9 to mediate efficient apical sorting. They raise the intriguing possibility that changes in glycosyltransferase expression patterns and/or galectin-9 distribution may acutely modulate endolyn trafficking in the kidney.**

Monitoring Editor
Keith E. Mostov
University of California, San Francisco

Received: Apr 30, 2012
Revised: Jul 11, 2012
Accepted: Jul 26, 2012

INTRODUCTION

Proper kidney function requires continuous regulation of protein trafficking and targeting in response to physiological stimuli. Ion transporters and other proteins necessary for renal function must be selectively targeted to the apical or basolateral cell surface of kidney cells and internalized or redistributed on demand to enable tightly controlled recovery of ions and metabolites from the renal filtrate. The polarity of epithelial cells is maintained by active sorting of newly synthesized and recycling proteins to the apical or basolateral membrane domains, which are kept physically separated by tight junctions. The signals and mechanisms that mediate this differential sorting of cargoes are both complex and diverse. Whereas basolateral sorting signals are typically linear peptide motifs, apical sorting signals are less well defined and can be present within the lumenal, transmembrane, or cytosolic regions of the protein (reviewed in Folsch *et al.*, 2009; Weisz and Rodriguez-Boulan, 2009). Protein association with glycolipid-enriched lipid rafts has been proposed to mediate apical sorting of some glycosylphosphatidylinositol-anchored proteins, as well as of the influenza transmembrane proteins hemagglutinin (HA) and neuraminidase. For other proteins, including megalin and several polytopic proteins, cytoplasmic peptide sequences direct apical targeting (Weisz and Rodriguez-Boulan, 2009). Finally, both N- and O-linked glycans within the lumenal

This article was published online ahead of print in MBoC in Press (http://www.molbiolcell.org/cgi/doi/10.1091/mbc.E12-04-0329) on August 1, 2012.

Address correspondence to: Ora A. Weisz (weisz@pitt.edu).

Abbreviations used: Gal, galectin; GlcNAcT, *N*-acetylglucosaminyltransferase; HA, influenza hemagglutinin; LEA, *Lycopersicon esculentum* agglutinin; MDCK, Madin–Darby canine kidney; MAA, *Maackia amurensis* agglutinin; SNA, *Sambucus nigra* agglutinin; TA, tetracycline transactivator; WGA, wheat germ agglutinin.

domains of some apical cargo have been demonstrated to function as apical targeting signals (reviewed in Rodriguez-Boulan and Gonzalez, 1999; Potter *et al.*, 2006a).

Two models have been proposed to mediate glycan-dependent sorting of apically destined cargoes (Rodriguez-Boulan and Gonzalez, 1999). First, glycans may somehow promote cargo clustering into sorting platforms by providing structural support. Alternatively, some proteins may be segregated for apical delivery upon binding to a sorting receptor that recognizes a carbohydrate-dependent epitope on the cargo. The carbohydrate-binding family of galectins (Gals) has been variously suggested to play a role in cargo sorting via both of these mechanisms. Gal-4 binding to sulfated galactosylceramides was shown to cause clustering of lipid rafts (Delacour *et al.*, 2005; Stechly *et al.*, 2009), whereas Gal-3 has been implicated in apical sorting of glycan-dependent cargoes that do not associate with lipid rafts (Delacour *et al.*, 2006, 2007, 2008). Madin–Darby canine kidney (MDCK) cells express Gal-3 > Gal-9 > Gal-8 > Gal-1 >> Gal-4 > Gal-7 > Gal-12 (Friedrichs *et al.*, 2007; Poland *et al.*, 2011). However, we found no effect of Gal-3 knockdown on the polarity of several glycan-dependent proteins, including endolyn, in MDCK cells (Mo *et al.*, 2010; Kinlough *et al.*, 2011; Mattila *et al.*, 2012).

Endolyn is a sialomucin that modulates cell adhesion, migration, and signaling in hematopoietic progenitor cells, myoblasts, and cancerous epithelial cells. Endolyn cycles constitutively from the cell surface to lysosomes and is selectively sorted to the apical surface of polarized kidney cells (Ihrke *et al.*, 2001, 2004; Potter *et al.*, 2006b). Although its function in either renal progenitor or in fully differentiated, polarized cells is unknown, we recently found that knockdown of endolyn in zebrafish embryos disrupted pronephric kidney morphology and function (Mo *et al.*, 2012). Moreover, these defects could be fully rescued by expression of rat endolyn but not by endolyn lacking apical membrane or lysosomal sorting determinants.

In polarized MDCK cells, newly synthesized and recycling endolyn is targeted apically via an N-glycan–dependent mechanism (Ihrke *et al.*, 2001; Potter *et al.*, 2004, 2006b). The lumenally exposed portion of endolyn contains two mucin domains linked by a disulfide-bonded compact domain. Rat endolyn contains eight N-glycosylation consensus sequences (Asn-X-Ser/Thr) and 40 predicted O-glycosylation sites (NetOglyc 3.1 program; Julenius *et al.*, 2005). Previous data from our lab revealed that disruption of two of the N-glycosylation sites within the disulfide-bonded domain (at positions 68 and 74) decreased the initial polarity of endolyn delivery to ~60–65% apical (compared with 75–80% apical for wild-type endolyn; Potter *et al.*, 2004). Mutagenesis of all eight N-glycosylation consensus sequences in endolyn resulted in nonpolarized delivery of the protein; however, apical sorting was fully rescued when N-glycosylation of Asn68 and Asn74 was restored (Potter *et al.*, 2004). Moreover, treatment of MDCK cells with deoxymannojirimycin or kifunensine, drugs that interfere with mannose trimming and subsequent terminal processing, fully disrupted apical delivery (Potter *et al.*, 2004). However, the specific glycan structure(s) required for endolyn apical delivery are unknown.

A common penultimate modification of both N- and O-glycans known to play important roles in protein sorting and cellular function is the addition of poly-*N*-acetyllactosamine (polylactosamine [PL]) chains to N- or O-glycans. These chains, consisting of repeating units of *N*-acetylglucosamine and galactose (GlcNAcβ1,4Gal), are added primarily to the β1,6 branch of multiantennary N-glycans. Availability of this site for PL addition is regulated by *N*-acetylglucosaminyltransferases (GlcNAcT) III and V (encoded by the GAT3 and GAT5 genes, respectively). These enzymes add or inhibit, respectively, the addition of the 1,6-linked *N*-acetylglucosamine, to which PL is typically added. Consequently, knockdown of GlcNAcT-III leads to enhanced branching and PL addition, whereas knockdown of GlcNAcT-V disrupts PL extension. Elegant studies by Dennis and colleagues demonstrated that PL addition regulated by these enzymes selectively modulates surface expression levels of a variety of cellular receptors (Lau *et al.*, 2007; Dennis *et al.*, 2009). Surface retention is apparently mediated by interaction of PL chains with Gal-3 (Lau *et al.*, 2007). In addition, knockdown of GlcNAcT-III or mutagenesis of N-glycans on the Na,K-ATPase β subunit was shown to disrupt the permeability barrier in MDCKs and led to alterations in cell adhesion, suggesting that epithelial cells can regulate the tightness of their cell junctions by modulating N-glycan branching (Vagin *et al.*, 2008).

Instead of PL chain addition, endolyn apical delivery could be modulated by sialylation of its N-glycans. Sialic acids are acidic sugars with a nine-carbon backbone, which can be commonly found on cell surface glycolipids and glycoproteins (Schauer, 2000). The variety of sialic acids is created by diverse α-linkages between the 2-carbon and the underlying sugars. The most common linkages on N-glycans are to the 3- or 6-position of galactose residues, termed α2,3 and α2,6 linkages, respectively. Members of a family of at least five different α2,3 sialyltransferases (ST3Gal-I–V) are responsible for synthesis of α2,3-linked sialic acids. The ST3Gal-III and ST3Gal-IV sialyltransferases are responsible for addition of α2,3-linked sialic acids to N-glycans, whereas only one sialyltransferase, ST6Gal-I, adds α2,6-linked sialic acids to N-glycans (Varki, 2009).

In this study, we dissected the requirements for endolyn N-glycosylation terminal processing that lead to apical sorting. Although we confirmed that endolyn N-glycans are modified by PL extension, modulation of PL addition by knockdown of GlcNAcT-III or -V did not affect the polarity of endolyn delivery. In contrast, we found that addition of both α2,3- and α2,6-linked sialic acids to endolyn N-glycans was essential for efficient apical delivery of endolyn. Knockdown of Gal-9, which bound with reduced affinity to endolyn synthesized in the presence of kifunensine, disrupted endolyn polarity in MDCK cells, suggesting that Gal-9 may selectively recognize sialylated glycans on endolyn to mediate its apical sorting.

RESULTS

The intracellular localization of endolyn varies along the renal tubule

Confocal immunofluorescence microscopy of rat kidney sections shows that endolyn is expressed in all segments of the renal tubule and in collecting duct. Its expression is particularly high in distal convoluted tubule and collecting duct, where it is largely confined to intracellular structures that contain the lysosomal marker lamp-1, consistent with endolyn's reported distribution throughout the endosomal and lysosomal system in various cultured cell types (Croze *et al.*, 1989; Ihrke *et al.*, 2000, 2001; Chan *et al.*, 2001). Surprisingly, in proximal convoluted tubule, endolyn is most concentrated at the apical surface (brush border) and/or in subapical vacuoles that contain little lamp-1 (Figure 1A). However, in proximal straight tubule and more distal nephron segments endolyn is absent from the apical surface and localizes to intracellular compartments, many of which correspond to lamp-1–rich lysosomes (Figure 1B). This suggests that endolyn traffics more efficiently to, or is better retained at, the apical surface in proximal convoluted tubule cells than in more distal tubular compartments.

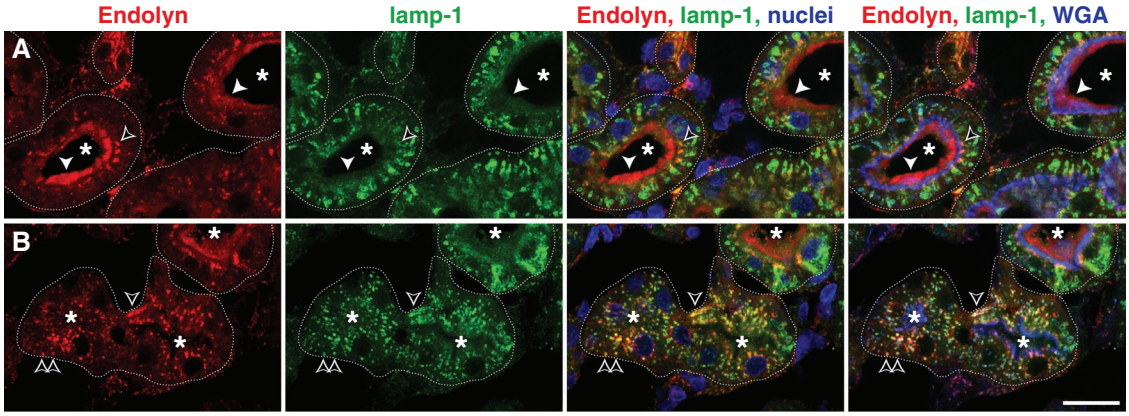

FIGURE 1: Endolyn is variously localized to the apical surface and endosomal/lysosomal compartments along the renal tubule. Paraformaldehyde-fixed rat kidney sections were labeled with antibodies to endolyn, the lysosomal membrane protein lamp-1, and WGA. Note the variable distribution of endolyn between the apical surface and endocytic compartments in different segments of the renal tubule. For easier identification, tubules are outlined at their basal aspect, and visible lumens are marked by asterisks. (A) Endolyn is seen prominently at the brush border (filled arrowheads) and subapical endosomes (open arrowhead) of S1 proximal convoluted tubules (PCTs). These tubules contain large lamp-1–positive lysosomes lateral and basal to their nuclei, which contain little endolyn. WGA labels the base of microvilli in PCT. A small portion of a distal convoluted tubule is seen at the top/middle of the image. (B) Endolyn is primarily intracellular in proximal straight tubule and more distal segments, where strong overlap with lamp-1 is evident. Open arrowheads point to lysosomes containing both proteins in a proximal straight tubule. Owing to the glancing and more longitudinal cut through this tubule, two stretches of the collapsed lumen are visible (marked by two asterisks). Note the presence of WGA and the absence of endolyn in the brush border of this tubule, in contrast to its apical presence in the adjacent PCT. Bar, 20 μm.

Apical delivery of endolyn is disrupted in ricin-resistant cells

Because endolyn's apical delivery is N-glycan dependent, differential terminal processing could explain its varied distribution along the renal tubule. To confirm that terminal processing of N-glycans is important for apical delivery of endolyn, we expressed the protein in ricin-resistant MDCK (MDCK-RCA) cells. These cells are deficient in UDP-galactose transport in the Golgi complex and thus lack the ability to add galactose to either N- and O-linked glycans, as well as to glycolipids. Consequently, N- and O-glycans lack terminal processing such as polylactosamine extension or sialylation. Despite these deficiencies, MDCK-RCA cells readily form polarized monolayers (Brandli *et al.*, 1988). Previous studies demonstrated that apical delivery of gp80 and lipid raft–associated proteins were not disrupted in MDCK-RCA cells, whereas the heavily glycosylated protein gp114 was partially missorted to the basolateral surface in these cells (Le Bivic *et al.*, 1993). Filter-grown MDCK-RCA or control cells were infected with replication-defective recombinant adenovirus expressing rat endolyn, radiolabeled with [^{35}S]Cys, and subjected to domain-selective biotinylation to assess the polarity of endolyn delivery. After biotinylation, cells were solubilized, and samples were immunoprecipitated using anti-endolyn antibody. After elution, one-fifth of the sample was reserved to quantify total endolyn, and the remainder was incubated with streptavidin-agarose to recover the biotinylated (surface) portion. Endolyn recovered from MDCK-RCA cells migrated more rapidly on SDS–PAGE compared with endolyn from control MDCK cells, consistent with altered glycan terminal processing (Figure 2A). As predicted, endolyn polarity was significantly disrupted in the MDCK-RCA cells (36% apical compared with 75% in control cells; Figure 2B). As a control experiment, we compared the polarity of influenza HA, a lipid raft–associated protein that is apically targeted via a glycan-independent mechanism, in MDCK and MDCK-RCA cells (Figure 1, C and D). Apical delivery of newly synthesized HA was similar in both cell lines.

Poly-*N*-acetyllactosamine extensions are not required for apical sorting of endolyn

As described, extension of N-linked glycans with PL chains is known to modulate glycoprotein surface expression and protein–protein interactions in several systems and is thus an attractive candidate to consider as a potential apical sorting signal on endolyn. To examine whether PL is important for endolyn sorting, we knocked down *N*-acetylglucosaminyltransferases GlcNAcT-III and GlcNAcT-V using small interfering RNAs (siRNAs) to enhance or reduce PL addition, respectively (Figure 3A). Knockdown was efficient, as determined by reverse transcriptase (RT)-PCR for GlcNAcT-III and GlcNAcT-V transcripts (Figure 3B). To test whether knockdown of these enzymes affected endolyn modification with PL, we radiolabeled with [^{35}S]Cys MDCK cells stably expressing endolyn and treated with the indicated siRNAs for 2 h. Endolyn was immunoprecipitated, and after recovery of endolyn from the immunoprecipitate, equal aliquots were incubated with either immobilized tomato lectin (*Lycopersicon esculentum* agglutinin [LEA]) or wheat germ (*Triticum vulgare*) agglutinin (WGA) or reserved to calculate total endolyn input. LEA recognizes polylactosamine, whereas WGA binds to the N-glycan chitobiose core structure Manβ1,4GlcNAcβ1,4GlcNAc as well as to sialic acid. As shown in Figure 3, C–E, WGA-conjugated beads captured ~70–80% of the total endolyn added, whereas only ~8% of endolyn recovered from control cells bound to LEA beads. Whereas the fraction of endolyn recovered by LEA- or WGA-conjugated beads was not increased in GlcNAcT-III–knockdown cells, knockdown of GlcNAcT-V significantly reduced recovery of endolyn on LEA beads and also increased the migration of endolyn on SDS gels (Figure 3C). Because both N- and O-linked glycans can be modified by PL extension, we also examined lectin binding of endolyn recovered from MDCK cells stably overexpressing the sialyltransferase ST6GalNAc-1 (ST6 cells), where PL extension of O-glycans is inhibited by preventing synthesis of all core O-glycans (Kinlough *et al.*,

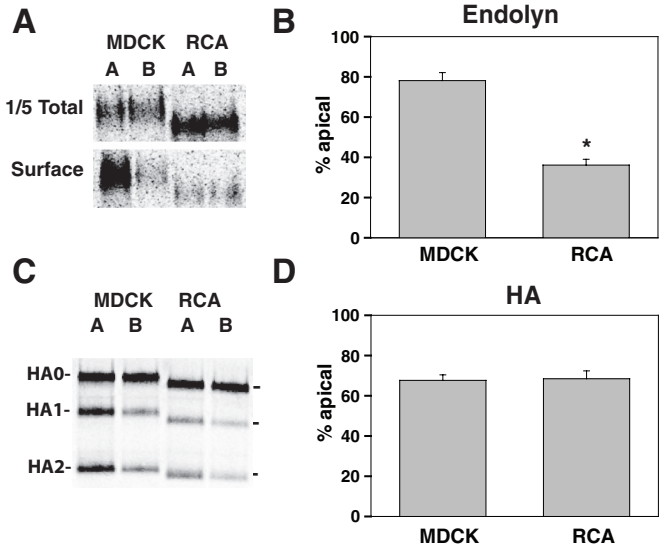

FIGURE 2: Endolyn polarity is selectively disrupted in ricin-resistant MDCK cells. (A) MDCK or MDCK-RCA cells were starved in cysteine-free medium for 30 min, radiolabeled with [^{35}S]Cys for 2 h, and chased for 1 h. The apical or basolateral surface of duplicate filters was biotinylated and the polarity of endolyn delivery was quantitated as described in *Materials and Methods*. A representative gel showing one-fifth of the total sample and streptavidin-bound (surface) endolyn recovered from apically (A) and basolaterally (B) biotinylated samples is shown. (B) Endolyn polarity quantitated from three independent experiments (mean ± SE) each performed in duplicate or triplicate. *$p = 0.003$ by Student's *t* test. (C) Polarized delivery of influenza HA was assessed using domain-selective trypsinization. MDCK or MDCK-RCA cells expressing HA were radiolabeled for 30 min with [^{35}S]Met/Cys and chased for 2 h, followed by apical or basolateral trypsinization and analysis as described in *Materials and Methods*. The migration of full-length HA (HA0) and HA trypsin fragments (HA1 and HA2) is noted. (D) The polarity (mean ± range) of HA quantitated from two independent experiments performed in duplicate.

2011). Approximately 8% of endolyn synthesized in ST6 cells bound to LEA beads, confirming that N-glycans on endolyn receive PL extension (Supplemental Figure S1). Together these data demonstrate that GlcNAcT-V knockdown decreases PL extension of N-glycans on endolyn.

To evaluate the effect of GlcNAcT knockdown on endolyn surface delivery, we radiolabeled polarized endolyn-expressing cells and subjected them to domain-selective surface biotinylation. As shown in Figure 4, polarized delivery of newly synthesized endolyn was not affected by either GlcNAcT-III or GlcNAcT-V knockdown. In addition, the total fraction of endolyn biotinylated under each condition was comparable (typically ~20%), suggesting that knockdown did not alter the efficiency of endolyn transit through the biosynthetic pathway. Similarly, no effects were observed on the steady-state distribution of endolyn assessed by indirect immunofluorescence (unpublished data). Thus PL extension on branched N-glycans is not required for endolyn apical delivery.

Sialylation of endolyn N-glycans is required for apical delivery

We next examined whether addition of sialic acids to the termini of endolyn N-glycans is important for apical sorting. To test whether endolyn contains α2,3- and/or α2,6-linked sialic acids, we incubated radiolabeled endolyn immunoprecipitated from polarized MDCK cells with the sialic acid–binding lectins *Maackia amurensis* agglutinin (MAA) and *Sambucus nigra* agglutinin (SNA), which specifically bind to α2,3 and α2,6 linkages, respectively. Whereas 73% of endolyn bound to MAA beads, only 16% was recovered on SNA beads (Figure 5, B and C, Ctrl), suggesting that the sialic acids on endolyn are predominantly in the α2,3 linkage. Additional experiments in which endolyn biotinylated at the apical or basolateral surface was recovered and incubated with lectin beads revealed that the apical and basolateral pools of endolyn had identical SNA and MAA binding profiles (unpublished data).

Next we knocked down ST3Gal-III, ST3Gal-IV, or ST6Gal-I (or various combinations) and examined the effect on sialylation of endolyn. Efficient knockdown of each enzyme was confirmed by RT-PCR analysis of transcript levels (Figure 5A) and the effects on glycan structures evaluated by lectin pull-down assays as described. Endolyn recovery on MAA beads tended to be lower when the enzymes responsible for α2,3 sialic acid addition (ST3Gal-III and IV) were knocked down individually, although these values were not significantly different from control. However, knockdown of both enzymes together (with or without concomitant ST6Gal-I knockdown to eliminate O-glycan synthesis) significantly reduced binding (from 73% in control to 35% upon double knockdown). As expected, knockdown of ST6Gal-I alone had no effect on endolyn binding to MAA (Figure 5, B and C). Conversely, only knockdown of ST6Gal-I (alone or in combination with knockdown of ST3Gal-III and ST3Gal-IV) significantly reduced binding of endolyn to SNA lectin. This demonstrates that N-glycans on endolyn are sialylated in both α2,3 and α2,6 linkages.

To examine the role of sialylation in endolyn apical sorting, we performed domain-selective cell surface biotinylation of endolyn in cells lacking the individual sialyltransferases described previously or combinations of all three (Figure 6). Knockdown of ST3Gal-III or ST3Gal-IV individually or together had no effect on the polarity of endolyn delivery. Similarly, depletion of ST6Gal-I was without effect on endolyn polarity. However, polarized endolyn delivery was significantly disrupted in cells depleted of all three sialyltransferases compared with cells transfected with control siRNA (48% apical in the triple knockdown cells compared with 75% in control cells).

To examine whether sialyltransferase knockdown caused a generic disruption in apical protein distribution, we examined the surface distribution of endolyn and two additional apical markers (influenza HA and the neurotrophin receptor p75) in control and knockdown cells using indirect immunofluorescence (Figure 7). Apical delivery of both HA and p75 is independent of N-linked glycosylation. Polarized apical delivery of p75 is conferred by the juxtamembrane O-glycosylated stalk domain of the protein (Yeaman *et al.*, 1997). All three proteins were tightly localized to the apical surface in polarized MDCK cells treated with control siRNA. As predicted, endolyn distribution was shifted in cells depleted of all three sialyltransferases, with considerable basolateral staining now evident. Of importance, tight junctions were apparently normal in these cells, as demonstrated by ZO-1 staining. In contrast, the apical distributions of HA and p75 were unaffected by sialyltransferase depletion. Overall these results suggest that sialylation of N-glycans is required for the apical biosynthetic delivery and steady-state distribution of endolyn but do not disrupt cell polarity in general.

Galectin-9 plays a role in apical sorting of endolyn

Members of the galectin family have been implicated in cell differentiation and apical protein sorting via several distinct mechanisms (Hikita *et al.*, 2000; Delacour *et al.*, 2005, 2007; Mishra *et al.*, 2010). MDCKs express several galectins, including Gal-1, -3, -4, -7,

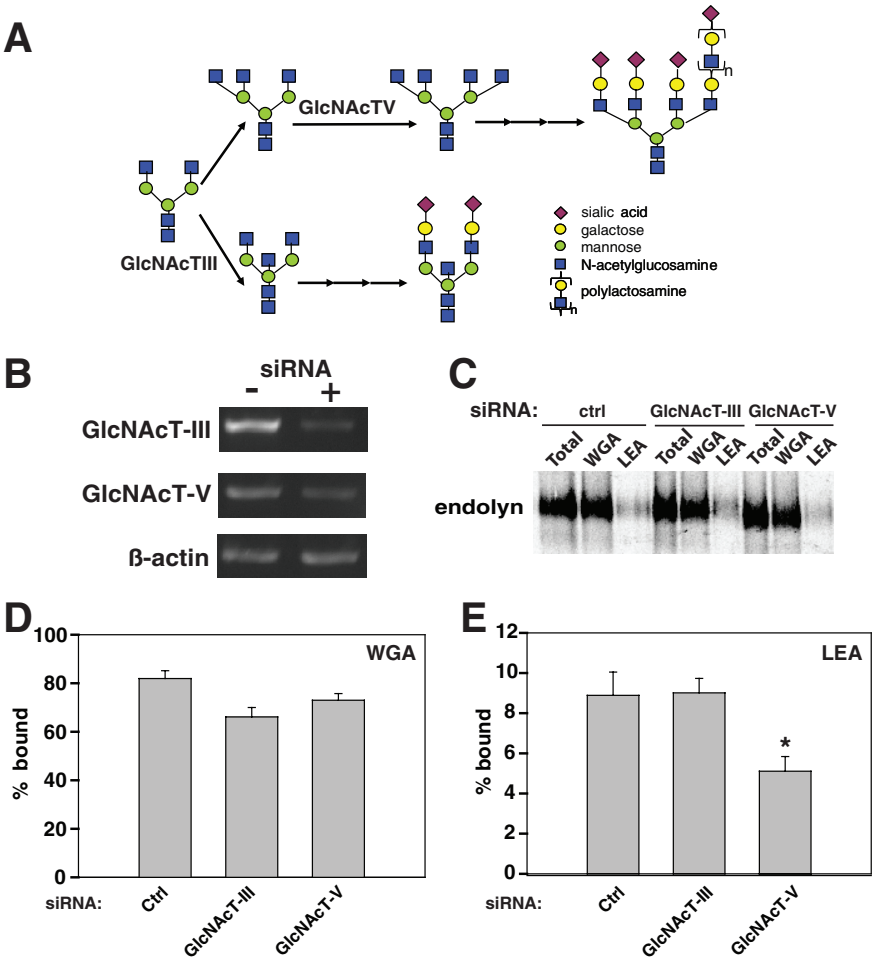

FIGURE 3: Modulation of GlcNAc transferase expression alters polylactosamine extension on endolyn glycans. (A) Schematic showing the effects of GlcNAcT-III and GlcNAcT-V expression on N-glycan branching and subsequent polylactosamine extension. GlcNAcT-III activity adds a bisecting GlcNAc to the β-mannose at the core position that prevents further branching and addition of PL. The competing enzyme GlcNAcT-V adds GlcNAc to the β1,6 branch, which allows polylactosamine extension during later processing steps. (B) Efficient knockdown of GlcNAc transferase enzymes that modulate N-glycan branching was verified by RT-PCR of MDCK cells transfected with either control siRNA or siRNA targeting GlcNAcT-III or GlcNAcT-V. RT-PCR to detect β-actin is shown as a control for input RNA levels. (C) Extracts from metabolically labeled, filter-grown MDCK cells expressing endolyn and transfected with either control siRNA or siRNA directed against GlcNAcT-III or GlcNAcT-V were immunoprecipitated with anti-endolyn antibodies. Bound fractions were eluted, and equal aliquots were incubated overnight with immobilized WGA or LEA or reserved as total before analysis by SDS–PAGE. Quantitation of endolyn binding to WGA-conjugated (D) or LEA-conjugated (E) agarose The mean ± SE of three independent experiments performed in duplicate is plotted. *$p < 0.05$ by Student's *t* test.

-8, -9, and -12 (Friedrichs *et al.*, 2007; Poland *et al.*, 2011). To see whether galectins might play a role in endolyn sorting, we tested the interaction of radiolabeled endolyn synthesized in the presence or absence of kifunensine (KIF; inhibits terminal N-glycan processing) with recombinant glutathione *S*-transferase–tagged canine galectins-1, -3, -4, -7, -8, -9N, and -9C bound to glutathione-conjugated beads as described in *Materials and Methods*. The N-terminal (9N) and C-terminal (9C) carbohydrate-recognition domains of Gal-9 were expressed separately due to aggregation of the recombinant full-length canine Gal-9 in bacteria (Poland *et al.*, 2011). Of interest, treatment with KIF dramatically reduced interaction of endolyn with galectins -3, -4, -7, and -9N (Supplemental Figure S2).

We previously showed that Gal-3 is not involved in endolyn delivery (Mo *et al.*, 2010), and Gal-7 has been localized on the primary cilium of polarized kidney epithelial cells, where it functions in ciliogenesis and wound healing (Rondanino *et al.*, 2011). We therefore knocked down Gal-4 and -9 and examined their effects on endolyn polarity. In addition, because Gal-8 selectively binds to sialic acid, we also tested the effect of Gal-8 knockdown on endolyn distribution. Knockdown of Gal-4 or Gal-8 was efficient based on RT-PCR analysis but had no effect on endolyn polarity monitored by indirect immunofluorescence or by domain-selective biotinylation (Supplemental Figure S3). Knockdown of Gal-9 was similarly efficient (Figure 8A) but resulted in statistically significant, although modest, redirection of newly synthesized endolyn to the basolateral surface (Figure 8, B and C). In contrast, biosynthetic delivery of influenza HA as measured by domain-selective trypsinization was unaffected by Gal-9 knockdown (Figure 8, D and E). Indirect immunofluorescence confirmed the partial redistribution of endolyn in Gal-9–depleted cells, whereas the steady-state localization of HA and p75 were unaffected (Figure 9). Similar results were obtained using another siRNA targeting a distinct sequence in Gal-9 (Supplemental Figure S4). Knockdown of galectins-3, -4, and -9 together had no additional effect on endolyn polarity compared with depletion of Gal-9 alone (control, 74.8 ± 2.3% apical vs. triple knockdown; 66.3 ± 1.6% apical; $p = 0.017$ by Student's *t* test). Because knockdown of Gal-9 in MDCK cells using lentiviral-expressed shRNA was reported to dramatically affect global cell polarity (Mishra *et al.*, 2010), we also monitored transepithelial resistance, the distribution of the tight junction marker ZO-1, and the polarity of the endogenously expressed apical protein gp135 (Supplemental Figure S5). None of these was altered in cells treated with siRNA targeting Gal-9 compared with control siRNA, indicating that the effects of Gal-9 depletion on endolyn delivery and distribution are not due to global perturbations in cell polarity. Thus Gal-9 has a mechanistic role in the N-glycan–dependent apical sorting of endolyn.

DISCUSSION

In this study we examined the determinants that mediate apical sorting of endolyn in polarized renal epithelial cells. Endolyn was delivered largely to the basolateral surface in ricin-resistant cells, which are unable to add terminal glycan modifications, consistent with our previous demonstration that terminal processing of N-glycans rather than the core N-glycan structures on endolyn are required for apical sorting (Potter *et al.*, 2004). Although we found that endolyn N-glycans exhibit PL extension, this modification is apparently not required for polarized delivery, as knockdown of the

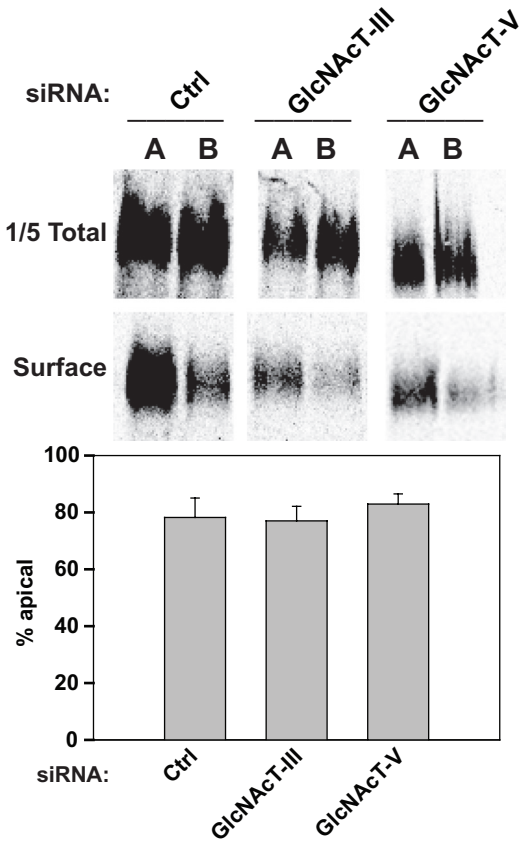

FIGURE 4: Biosynthetic delivery of endolyn is not affected by knockdown of GlcNAcT-III and GlcNAcT-V. Domain-selective biotinylation was performed on MDCK cells stably expressing rat endolyn and transfected with either control siRNA or siRNA targeting GlcNAcT-III or GlcNAcT-V as described in *Materials and Methods*. A representative gel showing one-fifth total and surface endolyn recovered from apically (A) and basolaterally (B) biotinylated samples is shown (top). Bottom, endolyn polarity (mean ± SE) quantitated from six independent experiments each performed in duplicate or triplicate. The total amount of endolyn biotinylated was similar in all cases (control, 22.9 ± 2.8% of total; GlcNAcT-III, 21.6 ± 2.5%; GlcNAcT-V, 23.6 ± 3.5%).

enzymes that modulate N-glycan branching and regulate PL addition had no effect on endolyn sorting. This finding is consistent with our previously reported observation that polarity of endolyn and other glycan-dependent apical proteins is unaffected by knockdown of Gal-3, which efficiently binds to PL chains (Mattila *et al.*, 2009; Mo *et al.*, 2010; Kinlough *et al.*, 2011). Instead, the presence of both α2,3- and α2,6-linked sialic acids on endolyn N-glycans was required for efficient apical sorting of the protein. Of interest, inhibition of endolyn terminal processing disrupted its binding to several canine galectins in vitro, and knockdown of Gal-9 (but not other galectins examined) selectively disrupted endolyn polarity. We conclude that Gal-9–mediated interaction with sialylated N-glycans on endolyn is important for apical targeting.

Sialic acid as an apical sorting determinant

Efficient apical sorting requires addition of either α2,3- and α2,6-linked sialic acids to endolyn N-glycans, as we observed defects in the polarity of delivery of newly synthesized endolyn, as well as the steady-state distribution, only when ST6Gal-I was knocked down in conjunction with ST3Gal-III and -IV. This suggests that a threshold level of sialic acid per se rather than the presence of specific linkages is sufficient to ensure sorting. Our lectin-binding studies measure binding to both N- and O-linked sialic acids, so changes in the levels of sialic acids on N-linked glycans cannot be directly assessed. However, knockdown of the sialyltransferases selective for N-linked glycans clearly affected binding to sialic acid–specific lectins and combined prevented polarized sorting of endolyn.

Sialylation of N- and O-glycans has previously been implicated in the sorting of other apical cargoes, including a secreted version of dipeptidylpeptidase IV (Slimane *et al.*, 2000). In addition, Real and colleagues suggested a role for sialylation in apical delivery of glycoproteins in HT-29 and Caco-2 cells (Huet *et al.*, 1998; Ulloa *et al.*, 2000). This conclusion was based on the observation that long-term treatment of cells with GalNAc-α-*O*-benzyl inhibits sialylation and causes intracellular retention of apically but not basolaterally destined proteins (Ulloa *et al.*, 2000; Delacour *et al.*, 2003).

How might sialic acids mediate apical sorting? It has been proposed that clustering of newly synthesized glycoproteins is a universal mechanism to sort apically designated cargoes (Weisz and Rodriguez-Boulan, 2009). It is possible that sialic acids facilitate the clustering or cross-linking of proteins into apical sorting platforms, either by enabling interactions between the cargo molecules or through binding to sorting receptors such as galectins. Sialylated N-glycans were been shown to be important for oligomerization of the serotonin transporter and its interaction with myosin IIA in CHO cells (Ozaslan *et al.*, 2003).

Mechanism of galectin-mediated sorting

Galectins may facilitate glycoprotein clustering and segregation, as they 1) recognize modified forms of a common structure present on both N- and O-glycans (PL), 2) form dimers or higher-order oligomers, and 3) are known to segregate glycoproteins into distinct membrane domains (Pace *et al.*, 1999).

How and where might binding to Gal-9 mediate endolyn sorting? Galectins are synthesized in the cytosol and exported from the cell via an unconventional and poorly understood secretion pathway. They can then bind to surface glycoconjugates and be internalized into endocytic compartments. Indeed, Gal-9 was found to bind selectively to the apically enriched Forssman glycolipid, and internalization studies following the trafficking of apically added Gal-9 revealed efficient retrograde transport to the *trans*-Golgi network, as well as to Rab11-positive compartments (Mishra *et al.*, 2010). As endolyn traffics through the apical recycling endosome (ARE) en route to the apical surface, it is conceivable that endolyn could bind to Gal-9 at either of these locations (Cresawn *et al.*, 2007). We previously showed that apical recycling of endolyn is disrupted when the apical surface pool of endolyn is desialylated (Potter *et al.*, 2006b). Thus Gal-9 might play a role in endolyn sorting in both the biosynthetic and the postendocytic pathway.

In a previously published study, MDCK cells depleted of Gal-9 using shRNA showed dramatic changes in cell morphology, polarity, and transepithelial resistance (TER; Mishra *et al.*, 2010). In contrast, under our Gal-9 depletion conditions, we did not observe any changes to cell structure, polarity, or TER other than reduced endolyn polarity. This may reflect a lower efficiency of Gal-9 depletion than that achieved by Mishra *et al.* (2010). Although our RT-PCR analysis confirmed essentially complete depletion of Gal-9 mRNA, we were unable to measure Gal-9 protein levels, as available antibodies did not recognize canine Gal-9.

Gal-9 contains two carbohydrate recognition domains (CRDs), and, intriguingly, only the N-terminal domain bound to endolyn in our in vitro studies. We speculate that differential glycan-binding

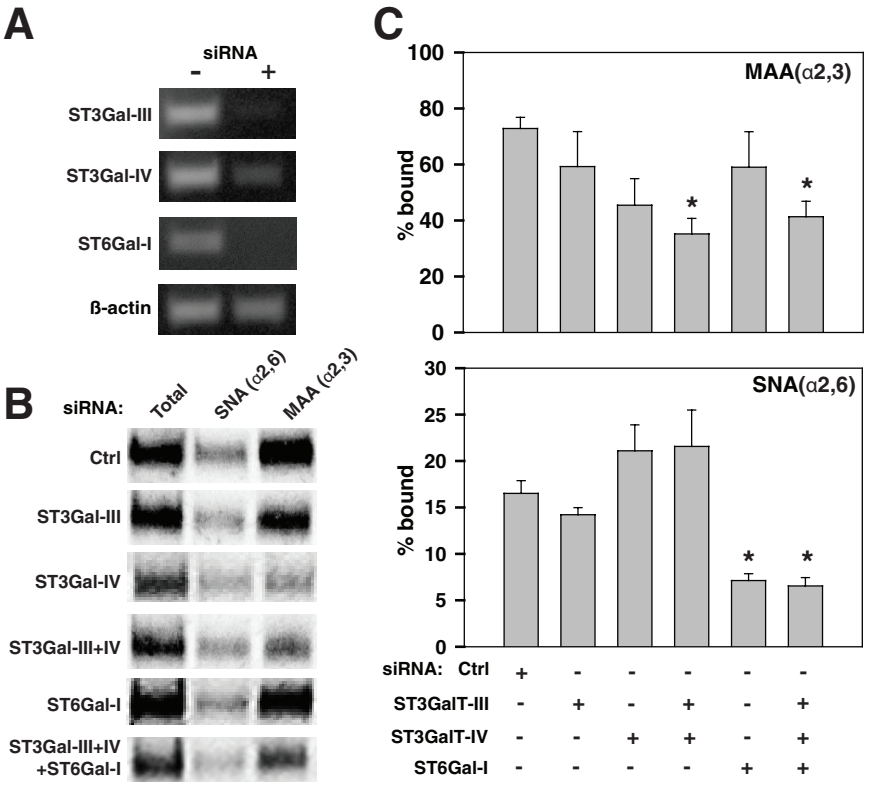

FIGURE 5: Endolyn contains both α2,3- and α2,6-linked sialic acids. MDCK cells were transfected with control siRNA or siRNA targeting ST3Gal-III, ST3Gal-IV, or ST6Gal-I in the indicated combinations. (A) RT-PCR of siRNA-treated MDCK cells demonstrates efficient knockdown of canine sialyltransferases. (B) Immunoprecipitates from endolyn expressing, metabolically labeled MDCK cells transfected with the indicated combinations of siRNAs were incubated overnight with SNA or MAA conjugated to agarose beads and then washed, and bound fractions were analyzed by SDS–PAGE. (C) Three independent experiments were quantified and plotted. *$p < 0.05$ compared with samples treated with control siRNA by Student's *t* test.

specificities of these domains may allow Gal-9 to be internalized using the C-terminal CRD (possibly by binding to the Forssman glycolipid) and interacting with cargo to be exported via the N-terminal CRD. Alternatively, the binding of Gal-9 to two distinct cargo proteins that have the intrinsic capacity to form dimers or oligomers could enable their cross-linking into a network able to recruit sorting machinery with high avidity. In support of this idea, there is evidence that endolyn can form dimers (Croze *et al.*, 1989).

Our findings that endolyn showed clear preference for binding Gal-9N and that blocking terminal N-glycan processing with KIF specifically reduced binding to Gal-9N led us to discover a role for Gal-9 in apical targeting of endolyn through knockdown experiments. However, our previous characterization of canine Gal-9N on a synthetic array of glycans did not reveal a preference for sialylated N-glycans. Instead, Gal-9N preferentially bound N-glycans with terminal blood group A and 3-O-sulfated disaccharides (Poland *et al.*, 2011). Because the array was created with synthetic glycans attached through various linkers to glass slides, it is possible that Gal-9N has additional preferences in a natural setting, such as that created by the two adjacent N-glycans on the disulfide loop of endolyn that we previously identified as critical for endolyn apical targeting. Alternatively, canine Gal-9N could have preference for a dog-specific, sialic acid–dependent N-linked structure expressed in MDCK cells. Future studies using a natural array created from MDCK cells should reveal any unique N-glycan structures (Song *et al.*, 2011).

Modulation of endolyn localization along the kidney tubule

Of interest, we find that endolyn distribution between apical and lysosomal compartments varies along the renal tubule, with pronounced apical localization in S1 of proximal convoluted tubule and more intracellular staining in more distal regions of the kidney. This distribution does not reflect the intrinsic endocytic capacity of renal tubular cells, as apical endocytosis is most highly developed in proximal convoluted tubule, precisely where endolyn surface expression is greatest. Instead, our observation that apical delivery of endolyn can be modulated by posttranslational N-glycan processing provides a possible explanation for its heterogeneous distribution. This raises the possibility that endolyn localization can be acutely modified by altering the expression or activity of enzymes involved in the synthesis or degradation of N-glycans. Indeed, a previous report documented differential recognition of human endolyn in various tissues using monoclonal antibodies directed toward distinct glycan-dependent epitopes on endolyn (Watt *et al.*, 2000). In the absence of a dominant apical sorting signal, endolyn would recycle more between lysosomes and the basolateral cell surface due to the presence of a cytosolic tyrosine-based motif (Ihrke *et al.*, 2000, 2004), and this could act in concert with a potentially reduced retention of endolyn at the apical surface. Alternatively, changes in Gal-9 expression might play a role in controlling the steady-state distribution of endolyn along the renal tubule; however, this is less likely, as Gal-9 is expressed throughout the cortex of adult mouse kidney (Wada *et al.*, 1997).

The expression patterns of sialyltransferases ST3GalT-III, ST3GalT-IV, and ST6Gal-I in the kidney have not been carefully examined. One previous report describes sialoconjugate distribution along the rat renal tubule assessed using SNA and MAA lectins (Zuber *et al.*, 2003). Of interest, this study found that only the α2,6-selective lectin SNA bound to the proximal convoluted tubule (S1 and S2 segments), whereas both SNA and MAA bound to the proximal straight tubule (S3). However, this approach cannot distinguish between sialic acids on N- versus O-linked glycans or on glycolipids and thus provides little information about sialyltransferase expression in these segments. Future studies will be directed toward determining how endolyn localization is differentially regulated in the kidney and the relevance of endolyn localization to its function in the developing and adult kidney.

MATERIALS AND METHODS

Immunofluorescence staining of rat kidney sections

Animal experiments were conducted under approved protocols by the Institutional Animal Care and Utilization Committee of the University of Pittsburgh, in accordance with the National Institutes of Health Guide for Care and Use of Laboratory Animals. The preparation and labeling of rat kidney cryostat sections has been

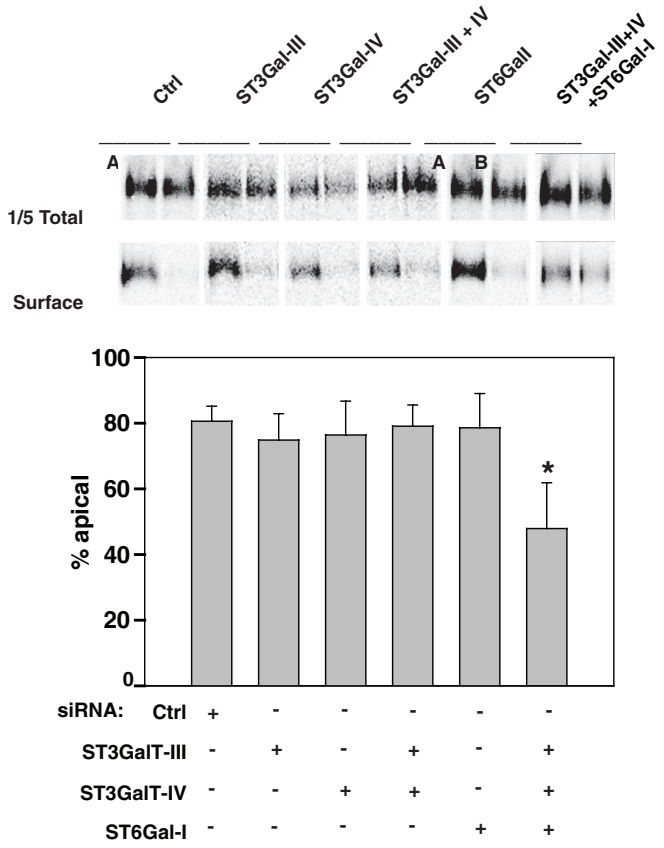

FIGURE 6: Both α2,3 and α2,6 sialic acid linkages are required for efficient apical delivery of endolyn. The polarity of endolyn delivery was assessed in MDCK cells transfected with either control siRNA or siRNA targeting ST3Gal-III, ST3Gal-IV, and ST6Gal-I as indicated. Top, representative gels showing total and surface (SA) endolyn recovered from apically (A) and basolaterally (B) biotinylated samples; bottom, endolyn polarity (mean ± SE) in three independent experiments each performed in duplicate or triplicate. *$p = 0.033$ by Student's t test.

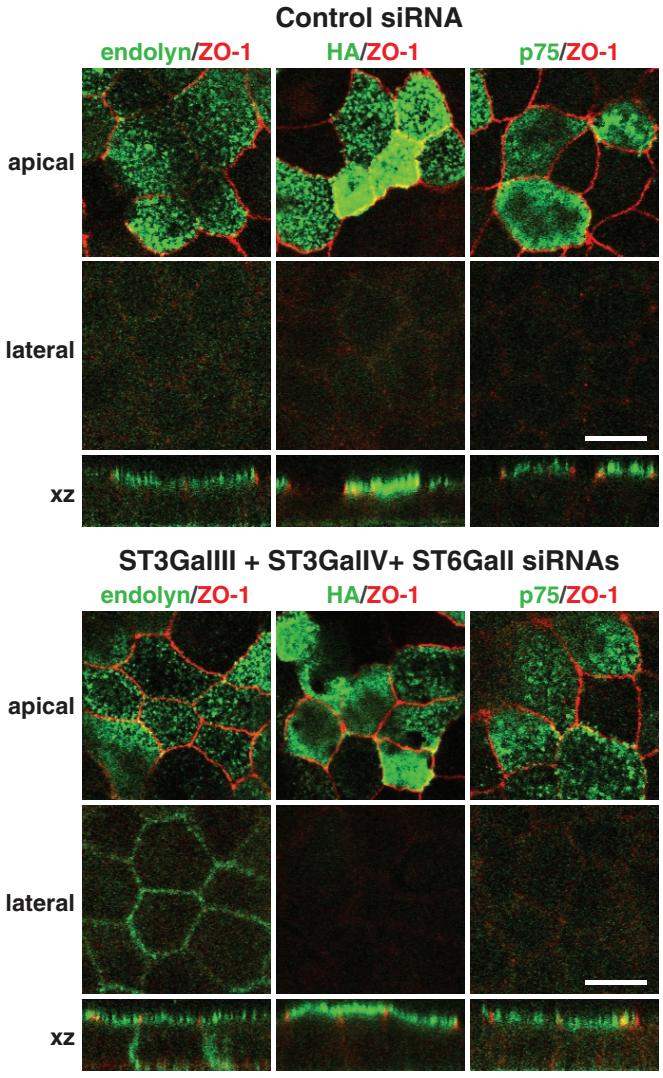

FIGURE 7: The steady-state surface distribution of endolyn is selectively disrupted in sialyltransferase-depleted cells. MDCK cells expressing endolyn, HA, or the neurotrophin receptor p75 were transfected with control siRNA or ST3Gal-III, ST3Gal-IV, and ST6Gal-I siRNA combinations as indicated and processed for surface labeling of the indicated protein (green) as described in *Materials and Methods*. Cells were then fixed and permeabilized and processed to detect the tight junction marker ZO-1 (red). Cells were imaged by confocal microscopy. Merged images of two *xy* sections (at apical and through the cell middle showing lateral staining, respectively) and one *xz* section are shown for each apical marker. Bar, 10 μm.

described (Rondanino *et al.*, 2011). Sections were colabeled with mouse monoclonal antibody GM10 (provided by Ken Siddle, University of Cambridge, Cambridge, United Kingdom; ascites 1:100; Grimaldi *et al.*, 1987) and rabbit serum 6431 to endolyn (1:200; Ihrke *et al.*, 2001), followed by DyLight 488–labeled donkey anti-mouse and Alexa 594–labeled donkey anti-rabbit secondary antibodies (Jackson ImmunoResearch Laboratories, West Grove, PA) and Alexa 647–conjugated WGA (Molecular Probes, Eugene, OR). Sections were mounted in Prolong Gold Antifade with 4′,6-diamidino-2-phenylindole (DAPI; Molecular Probes) to visualize nuclei. Optical sections 1 μm in size were imaged with a *z*-spacing of 0.5 μm using a Zeiss LSM 710 confocal microscope (Carl Zeiss, Jena, Germany) equipped with a Plan-Apochromat 63×/1.4 oil objective and processed using ImageJ (National Institutes of Health, Bethesda, MD) and Photoshop (Adobe, San Jose, CA) software. From 15 to 17 optical sections, corresponding to 7- to 8-μm tissue thickness, were projected by maximal fluorescence intensity.

Cell lines

MDCK II cells stably expressing rat endolyn were previously generated (Potter *et al.*, 2004). To maintain expression, cells were cultured in modified Eagle's medium (MEM, Sigma-Aldrich, St. Louis, CA) with 10% fetal bovine serum (FBS) and 400 μg/ml G418. Wild-type MDCK II cells and ricin-resistant cells (MDCK-RCA) were cultured in MEM supplemented with 10% FBS.

Antibodies

Mouse monoclonal antibodies 501 and 502 and rabbit polyclonal antibody 6431 (1:500 dilution for immunofluorescence) against rat endolyn were as described (Ihrke *et al.*, 1998, 2001). Antibodies 501 and 502 were used interchangeably and gave similar results. Hybridomas expressing anti-p75 and anti-HA were gifts from Enrique Rodriguez-Boulan (Weill Cornell Medical College) and Thomas Braciale (University of Virginia School of Medicine), respectively, and used at 1:1 dilution for immunofluorescence. Hybridoma supernatant expressing rat monoclonal anti–ZO-1 was provided by Gerard Apodaca (University of Pittsburgh School of Medicine) and used neat.

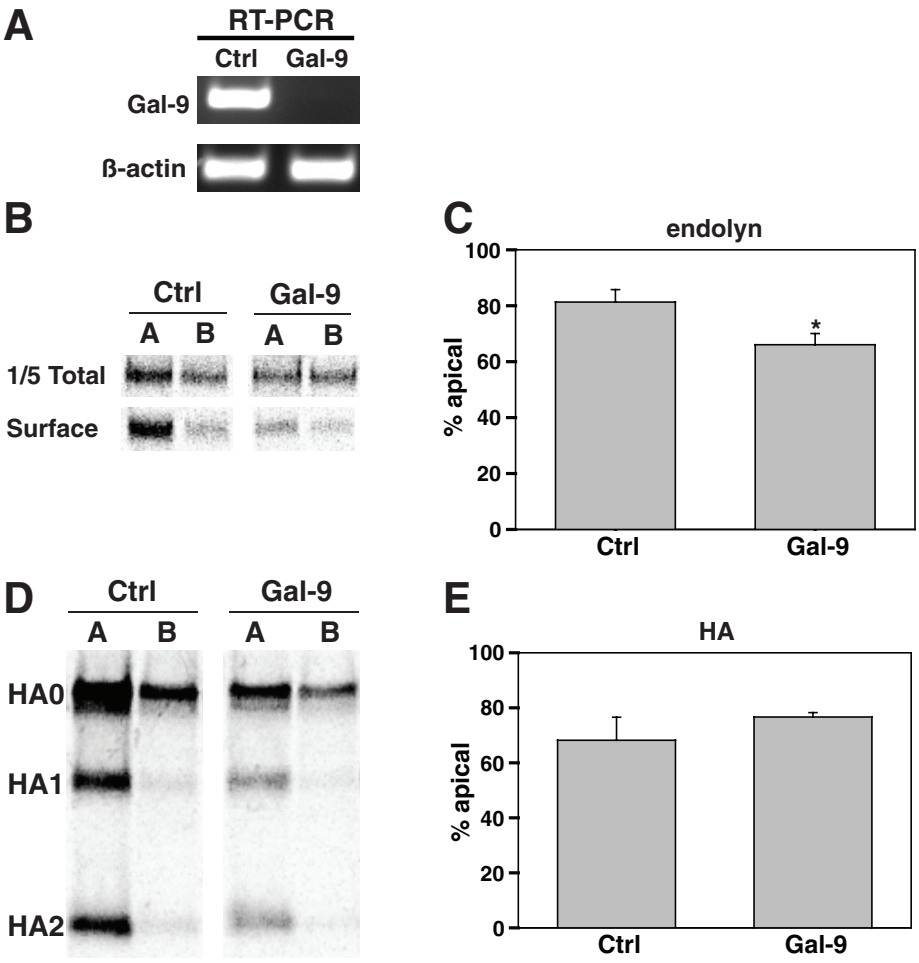

FIGURE 8: Knockdown of galectin-9 selectively disrupts endolyn polarity. MDCK cells were transfected with control or Gal-9 siRNA duplexes. (A) RT-PCR of siRNA-treated MDCK cells demonstrates efficient knockdown of canine Gal-9. The polarity of endolyn in MDCK cells transfected with either control siRNA or galectin-9 siRNA was assessed using domain-selective biotinylation as described in *Materials and Methods*. Representative gels are shown in B, and five independent experiments with duplicate or triplicate samples are plotted (mean ± SE; *p = 0.037 by Student's t test). (C). Polarized delivery of influenza HA was assessed as described in *Materials and Methods*. (D) The migration of full-length HA (HA0) and HA trypsin fragments (HA1 and HA2). (E) HA polarity.

Replication-defective recombinant adenoviruses and infection

Generation of replication-defective recombinant adenoviruses expressing influenza HA and rat endolyn using the Cre-Lox system has been previously described (Henkel and Weisz, 1998; Cresawn *et al.*, 2007). Adenovirus encoding the neurotrophin receptor p75 was originally provided by Enrique Rodriguez-Boulan. The tetracycline transactivator (TA) necessary for endolyn and HA expression was provided in-*trans* by coinfecting cells with an adenovirus expressing TA or by infecting MDCK cells stably expressing TA. Cells were incubated with adenoviruses at a multiplicity of infection of 50 as described in Henkel *et al*. (1998).

siRNA knockdown

siRNA duplex sequences targeting canine GlcNAcT-III and -V, ST3Gal-III and -IV, ST6Gal-I, and galectins-4, -8, and -9 are listed in Supplemental Table S1. For GlcNAcT-III and -V knockdown, siRNA duplexes (4–5 μg) suspended in 500 μl of Opti-MEM (GIBCO, Life Technologies, Carlsbad, CA) were incubated with 15 μl of Lipofectamine 2000 for 30 min at ambient temperature. The transfection mix (125 μl) and 5×10^5 MDCK cells in 333 μl of MEM were added to the upper chamber of a 12-well Transwell and triturated gently. Experiments were performed 4 d later. For ST3Gal-III and -IV and ST6Gal-I knockdown, 3–4 μg of siRNA duplex and 10 μl of Lipofectamine 2000 were used. For double and triple knockdown of sialyltransferases, 1–2 μg of each siRNA were mixed together, and 20 μl of Lipofectamine 2000 was used. For knockdown of galectins, 3-4 μg siRNA duplex and 15 μl Lipofectamine 2000 was used.

RT-PCR

RNA from MDCK cells treated with the indicated siRNAs was extracted using the RNAqueous phenol-free RNA isolation kit (Ambion, Austin, TX) according to the manufacturer's recommendations. Purified RNA (500 ng to 1 μg) was incubated with Moloney murine leukemia virus reverse transcriptase (Ambion) at 42°C for 1 h. PCR was set up after inactivation of reverse transcriptase using the GeneAmp High Fidelity PCR system (Applied Biosystems, Foster City, CA). Primers were designed to amplify a ~600–base pair sequence within each targeted protein and a ~200–base pair sequence within β-actin. The denaturing temperature was 95°C, the annealing temperature was 55°C, and the extension temperature was 68°C, with an amplification cycle of 25.

Domain-selective biotinylation

Domain-selective biotinylation was performed as previously described (Mo *et al*. 2010). Briefly, MDCK II cells were grown on filters for 4 d after transfection with the indicated siRNA duplexes. Cells were starved in cysteine-free medium for 30 min, radiolabeled for 2 h with [^{35}S]cysteine (MP Biomedicals, Solon, OH), and then chased in 4-(2-hydroxyethyl)-1-piperazineethanesulfonic acid (HEPES)–buffered MEM for 1 h before apical or basolateral biotinylation. Cells were solubilized, and lysates were immunoprecipitated with monoclonal anti-endolyn antibody 501 or 502. After recovery of antibody–antigen complexes, one-fifth of each sample was reserved to calculate the total recovery, and the remainder was incubated with streptavidin to recover biotinylated proteins. Samples were resolved on SDS–PAGE, and biotinylation efficiency was quantitated using a PhosphorImager (Bio-Rad, Hercules, CA). Statistical significance was analyzed using Student's t test.

Surface delivery of HA

Wild-type MDCK or MDCK-RCA cells were plated on permeable supports for 3 d before coinfection with adenoviruses encoding HA and TA. HA trypsinization was performed essentially as previously described (Henkel and Weisz, 1998). Briefly, cells were starved for 30 min, radiolabeled for 30 min, and chased for 2 h. Cells were rapidly chilled on ice, rinsed with ice-cold phosphate-buffered saline (PBS), and incubated with apically or basolaterally added 100 μg/ml

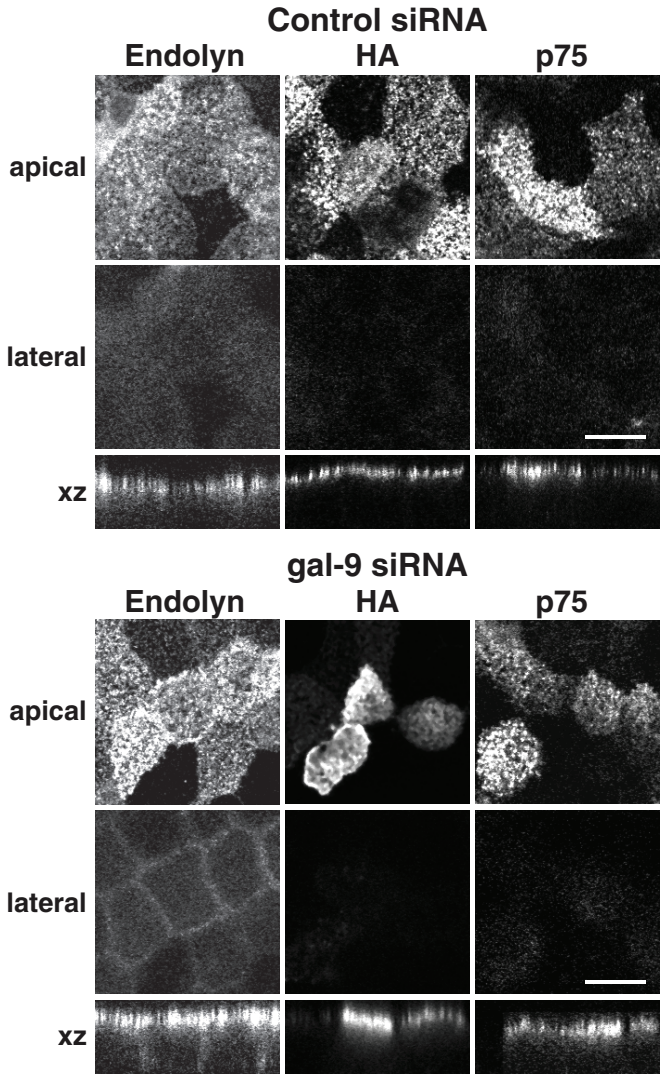

FIGURE 9: Knockdown of galectin-9 selectively alters the steady-state surface distribution of endolyn. MDCK cells transfected with control or Gal-9 siRNA duplexes were grown on filter supports for 3 d and then infected with replication-defective recombinant adenoviruses encoding endolyn, HA, or p75. Cells were processed to detect surface proteins as described in *Materials and Methods* and imaged using confocal microscopy. Representative *xy* sections through apical and middle ("lateral") planes and *xz* sections are shown. Bar, 10 µm.

N-tosyl-L-phenylalanine chloromethyl ketone–trypsin (Sigma-Aldrich) for 30 min and then with 200 µg/ml soybean trypsin inhibitor (Sigma-Aldrich). One sample was left untrypsinized to determine background proteolysis of HA, and this value (typically <5%) was subtracted from all samples. After lysis, full-length HA (HA0) and the two disulfide-bonded cleavage products (HA1 and HA2) were immunoprecipitated using monoclonal antibody Fc125. Samples were resolved on SDS–PAGE, and the percentage of HA accessible to cleavage at either surface domain was quantitated to determine polarity.

Immunofluorescence microscopy

Filter-grown MDCK cells were washed with chilled HEPES-buffered MEM for 15 min and blocked with HEPES-buffered MEM containing bovine serum albumin and 10% FBS for 15 min. To detect surface proteins, cells were incubated with primary antibodies for 1 h on ice, washed extensively, and then incubated with Alexa 488–conjugated goat secondary antibodies (1:500; Invitrogen, Carlsbad, CA) for 30 min on ice. After extensive washing, cells were fixed with 4% paraformaldehyde for 15 min at room temperature and permeabilized with 0.1% Triton X-100 in PBS-containing glycine and NH_4Cl at ambient temperature for 5 min. Permeabilized cells were incubated sequentially with rat anti–ZO-1 hybridoma supernatant for 30 min at 37°C and Alexa 647–conjugated secondary antibody (1:500; Invitrogen) for 30 min at ambient temperature. Filters were mounted onto slides using ProLong Gold Antifade Reagent with DAPI (Invitrogen). Confocal images were acquired using a Leica TCS SP microscope (Leica, Wetzlar, Germany) equipped with a 100× HCX PL-APO objective and processed using MetaMorph (Molecular Devices, Sunnyvale, CA) and Photoshop software.

Lectin-binding assays

Polarized MDCK cells stably expressing endolyn and transfected with the indicated siRNA duplexes were metabolically labeled with [^{35}S]Cys for 2 h and chased for 1 h. After immunoprecipitation, samples were eluted in 2% SDS, diluted with RIPA buffer, and incubated with 50 µl of the indicated lectin-agarose beads (EY Laboratories, San Mateo, CA). For LEA and WGA lectin binding, eluted samples were divided into three aliquots, one of which was reserved as "total." For SNA and MAA lectin binding, one-fifth of each sample was reserved to calculate the total immunoprecipitate, and the remainder was divided equally for incubation with immobilized lectins as indicated. Samples were incubated with lectin beads overnight at 4°C with end-over-end mixing, washed gently one time with RIPA buffer, and analyzed by SDS–PAGE.

ACKNOWLEDGMENTS

We thank Paul Poland and Carol Truschel for expert technical assistance. We are grateful to Gerard Apodaca, Enrique Rodriguez-Boulan, Ken Siddle, and Thomas Braciale for gifts of antibodies, hybridomas, and adenovirus. This work was supported by National Institutes of Health Grants DK54407 (to O.A.W.), DK54787 (to R.P.H.), and AHA 12SDG8960000 (to R.T.Y.) and by a grant-in-aid award from the National Kidney Foundation (NKF/NCA) to G.I. S.A.C. was supported in part by Howard Hughes Medical Institute Summer Scholarship 52006917. We are grateful to the Urinary Tract Epithelial Imaging and Physiology Cores of the P30 Pittsburgh Center for Kidney Research (National Institutes of Health DK079307) for assistance.

REFERENCES

Brandli AW, Hansson GC, Rodriguez-Boulan E, Simons K (1988). A polarized epithelial cell mutant deficient in translocation of UDP-galactose into the Golgi complex. J Biol Chem 263, 16283–16290.

Chan JY, Lee-Prudhoe JE, Jorgensen B, Ihrke G, Doyonnas R, Zannettino AC, Buckle VJ, Ward CJ, Simmons PJ, Watt SM (2001). Relationship between novel isoforms, functionally important domains, and subcellular distribution of CD164/endolyn. J Biol Chem 276, 2139–2152.

Cresawn KO, Potter BA, Oztan A, Guerriero CJ, Ihrke G, Goldenring JR, Apodaca G, Weisz OA (2007). Differential involvement of endocytic compartments in the biosynthetic traffic of apical proteins. EMBO J 26, 3737–3748.

Croze E, Ivanov IE, Kreibich G, Adesnik M, Sabatini DD, Rosenfeld MG (1989). Endolyn-78, a membrane glycoprotein present in morphologically diverse components of the endosomal and lysosomal compartments—implications for lysosome biogenesis. J Cell Biol 108, 1597–1613.

Delacour D, Cramm-Behrens CI, Drobecq H, Le Bivic A, Naim HY, Jacob R (2006). Requirement for galectin-3 in apical protein sorting. Curr Biol 16, 408–414.

Delacour D, Gouyer V, Leteurtre E, Ait-Slimane T, Drobecq H, Lenoir C, Moreau-Hannedouche O, Trugnan G, Huet G (2003). 1-Benzyl-2-acetamido-2-deoxy-alpha-D-galactopyranoside blocks the apical biosynthetic pathway in polarized HT-29 cells. J Biol Chem 278, 37799–37809.

Delacour D *et al.* (2005). Galectin-4 and sulfatides in apical membrane trafficking in enterocyte-like cells. J Cell Biol 169, 491–501.

Delacour D, Greb C, Koch A, Salomonsson E, Leffler H, Le Bivic A, Jacob R (2007). Apical sorting by galectin-3-dependent glycoprotein clustering. Traffic 8, 379–388.

Delacour D, Koch A, Ackermann W, Eude-Le Parco I, Elsasser HP, Poirier F, Jacob R (2008). Loss of galectin-3 impairs membrane polarisation of mouse enterocytes in vivo. J Cell Sci 121, 458–465.

Dennis JW, Lau KS, Demetriou M, Nabi IR (2009). Adaptive regulation at the cell surface by N-glycosylation. Traffic 10, 1569–1578.

Folsch H, Mattila PE, Weisz OA (2009). Taking the scenic route: biosynthetic traffic to the plasma membrane in polarized epithelial cells. Traffic 10, 972–981.

Friedrichs J, Torkko JM, Helenius J, Teravainen TP, Fullekrug J, Muller DJ, Simons K, Manninen A (2007). Contributions of galectin-3 and -9 to epithelial cell adhesion analyzed by single cell force spectroscopy. J Biol Chem 282, 29375–29383.

Grimaldi KA, Hutton JC, Siddle K (1987). Production and characterization of monoclonal antibodies to insulin secretory granule membranes. Biochem J 245, 557–566.

Henkel JR, Apodaca G, Altschuler Y, Hardy S, Weisz OA (1998). Selective perturbation of apical membrane traffic by expression of influenza M2, an acid-activated ion channel, in polarized madin-darby canine kidney cells. Mol Biol Cell 9, 2477–2490.

Henkel JR, Weisz OA (1998). Influenza virus M2 protein slows traffic along the secretory pathway. pH perturbation of acidified compartments affects early Golgi transport steps. J Biol Chem 273, 6518–6524.

Hikita C, Vijayakumar S, Takito J, Erdjument-Bromage H, Tempst P, Al-Awqati Q (2000). Induction of terminal differentiation in epithelial cells requires polymerization of hensin by galectin 3. J Cell Biol 151, 1235–1246.

Huet G *et al.* (1998). GalNAc-alpha-O-benzyl inhibits NeuAcalpha2-3 glycosylation and blocks the intracellular transport of apical glycoproteins and mucus in differentiated HT-29 cells. J Cell Biol 141, 1311–1322.

Ihrke G, Bruns JR, Luzio JP, Weisz OA (2001). Competing sorting signals guide endolyn along a novel route to lysosomes in MDCK cells. EMBO J 20, 6256–6264.

Ihrke G, Gray SR, Luzio JP (2000). Endolyn is a mucin-like type I membrane protein targeted to lysosomes by its cytoplasmic tail. Biochem J 345 Pt 2, 287–296.

Ihrke G, Kyttala A, Russell MR, Rous BA, Luzio JP (2004). Differential use of two AP-3-mediated pathways by lysosomal membrane proteins. Traffic 5, 946–962.

Ihrke G, Martin GV, Shanks MR, Schrader M, Schroer TA, Hubbard AL (1998). Apical plasma membrane proteins and endolyn-78 travel through a subapical compartment in polarized WIF-B hepatocytes. J Cell Biol 141, 115–133.

Julenius K, Molgaard A, Gupta R, Brunak S (2005). Prediction, conservation analysis, and structural characterization of mammalian mucin-type O-glycosylation sites. Glycobiology 15, 153–164.

Kinlough CL, Poland PA, Gendler SJ, Mattila PE, Mo D, Weisz OA, Hughey RP (2011). Core-glycosylated mucin-like repeats from MUC1 are an apical targeting signal. J Biol Chem 286, 39072–39081.

Lau KS, Partridge EA, Grigorian A, Silvescu CI, Reinhold VN, Demetriou M, Dennis JW (2007). Complex N-glycan number and degree of branching cooperate to regulate cell proliferation and differentiation. Cell 129, 123–134.

Le Bivic A, Garcia M, Rodriguez-Boulan E (1993). Ricin-resistant Madin-Darby canine kidney cells missort a major endogenous apical sialoglycoprotein. J Biol Chem 268, 6909–6916.

Mattila PE, Kinlough CL, Bruns JR, Weisz OA, Hughey RP (2009). MUC1 traverses apical recycling endosomes along the biosynthetic pathway in polarized MDCK cells. Biol Chem 390, 551–556.

Mattila PE, Youker RT, Mo D, Bruns JR, Cresawn KO, Hughey RP, Ihrke G, Weisz OA (2012). Multiple biosynthetic trafficking routes for apically secreted proteins in MDCK cells. Traffic 13, 433–442.

Mishra R, Grzybek M, Niki T, Hirashima M, Simons K (2010). Galectin-9 trafficking regulates apical-basal polarity in Madin-Darby canine kidney epithelial cells. Proc Natl Acad Sci USA 107, 17633–17638.

Mo D, Ihrke G, Costa SA, Brilli L, Labilloy A, Halfter W, Cianciolo Cosentino C, Hukriede NA, Weisz OA (2012). Apical targeting and endocytosis of the sialomucin endolyn are essential for establishment of zebrafish pronephric kidney function. J Cell Sci (*in press*).

Mo D, Potter BA, Bertrand CA, Hildebrand JD, Bruns JR, Weisz OA (2010). Nucleofection disrupts tight junction fence function to alter membrane polarity of renal epithelial cells. Am J Physiol Renal Physiol 299, F1178–F1184.

Ozaslan D, Wang S, Ahmed BA, Kocabas AM, McCastlain JC, Bene A, Kilic F (2003). Glycosyl modification facilitates homo- and hetero-oligomerization of the serotonin transporter. A specific role for sialic acid residues. J Biol Chem 278, 43991–44000.

Pace KE, Lee C, Stewart PL, Baum LG (1999). Restricted receptor segregation into membrane microdomains occurs on human T cells during apoptosis induced by galectin-1. J Immunol 163, 3801–3811.

Poland PA, Rondanino C, Kinlough CL, Heimburg-Molinaro J, Arthur CM, Stowell SR, Smith DF, Hughey RP (2011). Identification and characterization of endogenous galectins expressed in Madin Darby canine kidney cells. J Biol Chem 286, 6780–6790.

Potter BA, Hughey RP, Weisz OA (2006a). Role of N- and O-glycans in polarized biosynthetic sorting. Am J Physiol Cell Physiol 290, C1–C10.

Potter BA, Ihrke G, Bruns JR, Weixel KM, Weisz OA (2004). Specific N-glycans direct apical delivery of transmembrane, but not soluble or glycosylphosphatidylinositol-anchored forms of endolyn in Madin-Darby canine kidney cells. Mol Biol Cell 15, 1407–1416.

Potter BA, Weixel KM, Bruns JR, Ihrke G, Weisz OA (2006b). N-glycans mediate apical recycling of the sialomucin endolyn in polarized MDCK cells. Traffic 7, 146–154.

Rodriguez-Boulan E, Gonzalez A (1999). Glycans in post-Golgi apical targeting: sorting signals or structural props? Trends Cell Biol 9, 291–294.

Rondanino C *et al.* (2011). Galectin-7 modulates the length of the primary cilia and wound repair in polarized kidney epithelial cells. Am J Physiol. Ren Physiol 301, F622–F633.

Schauer R (2000). Achievements and challenges of sialic acid research. Glycoconj J 17, 485–499.

Slimane TA, Lenoir C, Sapin C, Maurice M, Trugnan G (2000). Apical secretion and sialylation of soluble dipeptidyl peptidase IV are two related events. Exp Cell Res 258, 184–194.

Song X, Heimburg-Molinaro J, Smith DF, Cummings RD (2011). Derivatization of free natural glycans for incorporation onto glycan arrays: derivatizing glycans on the microscale for microarray and other applications. Curr Protoc Chem Biol 3, 53–63.

Stechly L *et al.* (2009). Galectin-4-regulated delivery of glycoproteins to the brush border membrane of enterocyte-like cells. Traffic 10, 438–450.

Ulloa F, Franci C, Real FX (2000). GalNAc-alpha-O-benzyl inhibits sialylation of de novo synthesized apical but not basolateral sialoglycoproteins and blocks lysosomal enzyme processing in a post-*trans*-Golgi network compartment. J Biol Chem 275, 18785–18793.

Vagin O, Tokhtaeva E, Yakubov I, Shevchenko E, Sachs G (2008). Inverse correlation between the extent of N-glycan branching and intercellular adhesion in epithelia. Contribution of the Na,K-ATPase beta1 subunit. J Biol Chem 283, 2192–2202.

Varki A (2009). Essentials of Glycobiology, Cold Spring Harbor, NY: Cold Spring Harbor Laboratory Press, Chapter 13.

Wada J, Ota K, Kumar A, Wallner EI, Kanwar YS (1997). Developmental regulation, expression, and apoptotic potential of galectin-9, a beta-galactoside binding lectin. J Clin Invest 99, 2452–2461.

Watt SM *et al.* (2000). Functionally defined CD164 epitopes are expressed on CD34(+) cells throughout ontogeny but display distinct distribution patterns in adult hematopoietic and nonhematopoietic tissues. Blood 95, 3113–3124.

Weisz OA, Rodriguez-Boulan E (2009). Apical trafficking in epithelial cells: signals, clusters and motors. J Cell Sci 122, 4253–4266.

Yeaman C, Le Gall AH, Baldwin AN, Monlauzeur L, Le Bivic A, Rodriguez-Boulan E (1997). The O-glycosylated stalk domain is required for apical sorting of neurotrophin receptors in polarized MDCK cells. J Cell Biol 139, 929–940.

Zuber C, Paulson JC, Toma V, Winter HC, Goldstein IJ, Roth J (2003). Spatiotemporal expression patterns of sialoglycoconjugates during nephron morphogenesis and their regional and cell type-specific distribution in adult rat kidney. Histochem Cell Biol 120, 143–160.